



HAL
open science

An immersed interface method for the solution of the standard parabolic equation in range-dependent ocean environments

Roberto Sabatini, Paul Cristini

► **To cite this version:**

Roberto Sabatini, Paul Cristini. An immersed interface method for the solution of the standard parabolic equation in range-dependent ocean environments. *Journal of the Acoustical Society of America*, 2018, 143 (4), pp.EL243. 10.1121/1.5029394 . hal-01624959

HAL Id: hal-01624959

<https://hal.science/hal-01624959>

Submitted on 26 Oct 2017

HAL is a multi-disciplinary open access archive for the deposit and dissemination of scientific research documents, whether they are published or not. The documents may come from teaching and research institutions in France or abroad, or from public or private research centers.

L'archive ouverte pluridisciplinaire **HAL**, est destinée au dépôt et à la diffusion de documents scientifiques de niveau recherche, publiés ou non, émanant des établissements d'enseignement et de recherche français ou étrangers, des laboratoires publics ou privés.



Distributed under a Creative Commons Attribution 4.0 International License

**An immersed interface method for the solution of the standard
parabolic equation in range-dependent ocean environments**

Roberto Sabatini^{a)} and Paul Cristini

Aix Marseille Univ, CNRS, Centrale Marseille, LMA, Marseille, France

sabatini@lma.cnrs-mrs.fr, cristini@lma.cnrs-mrs.fr

(Dated: 26 October 2017)

1 **Abstract:** A novel approach for the treatment of irregular ocean
2 bottoms within the framework of the standard parabolic equation is
3 proposed. The present technique is based on the immersed interface
4 method originally developed by LeVeque and Li [SIAM J. Numer. Anal.
5 **31**(4), 1019–1044, (1994)]. It is intrinsically energy-conserving and al-
6 lows to naturally handle generic range-dependent bathymetries, with-
7 out requiring any additional specific numerical procedure. An illus-
8 tration of its capabilities is provided by solving the well-known wedge
9 problem.

© 2017 Acoustical Society of America.

^{a)} Author to whom correspondence should be addressed.

1. Introduction

Propagation models based on different types of parabolic equations have been extensively used during the last four decades in underwater acoustics. Interested readers can find an exhaustive review in the book of [Jensen *et al.* \(2011\)](#) as well as in the paper of [Xu *et al.* \(2016\)](#). Since the earliest investigations of ocean sound propagation, one of the main issues has been related to the correct treatment of the interface between the water column and the seabed. Indeed, when solving a parabolic equation by approximating the seafloor as a series of stair-steps, a fundamental problem of energy conservation arises (see [Jensen *et al.* \(2011\)](#) and references therein). Current methods which allow to properly handle range-dependent bottoms essentially include: stair-step approximations within energy-conserving parabolic models ([Collins and Westwood, 1991](#)); domain rotations ([Collins, 1990](#)); and mapping techniques ([Metzler *et al.*, 2014](#)). In this letter, a novel approach, based on the immersed interface method (IIM) originally developed by [LeVeque and Li \(1994\)](#), is proposed. The parabolic equation is solved on a regular Cartesian grid, in which the bathymetry is “immersed”. Away from the bottom interface, standard centered finite difference schemes are employed to compute the derivatives along the vertical axis and the Crank-Nicolson method is used for the integration in range. Conversely, at grid points lying across the bottom, the aforementioned numerical schemes are slightly modified in order for the acoustic field to satisfy not only the governing equation but also the physical interface conditions. As a result, the proposed approach is intrinsically energy-conserving and allows to handle generic range-dependent ocean

30 bottoms. Therefore, it can be viewed as a generalization of the IFD method developed by
 31 [Lee and McDaniel \(1988\)](#).

32 In this letter, the new technique is developed for the standard parabolic equation and
 33 for fluid-fluid interfaces. Extensions to more wide-angle parabolic equations and to fluid-
 34 solid interfaces will be considered in future works. The letter is organized as follows: after
 35 a brief review of the standard parabolic model (Section 2), the new method is presented
 36 (Section 3); an example of application is then described (Section 4); concluding remarks are
 37 finally drawn.

38 2. The standard parabolic equation and interface conditions

39 In the context of this work, wave propagation is assumed to be azimuthally symmetric. A
 40 cylindrical coordinate system Orz , with the origin O on the sea surface, is thus considered.
 41 The bottom interface $z = \xi(r)$ is supposed to be irregular and the seabed is modeled as an
 42 equivalent fluid medium. A point source is placed on the z -axis at depth z_s . A sketch of
 43 the problem is illustrated in Fig. 1. In both the water column (medium 1) and the seabed
 45 (medium 2), the acoustic field in the far field can be described, in the frequency domain, by
 46 the standard parabolic equation¹ ([Jensen *et al.*, 2011](#))

$$\psi_r = \mathcal{F}, \quad \mathcal{F} = \frac{ik_0}{2} (\varepsilon^2 - 1) \psi + \frac{i}{2k_0} \psi_{zz}, \quad (1)$$

47 with $\hat{p}'(r, z) = \psi(r, z)\mathcal{H}_0^{(1)}(k_0 r)$, where \hat{p}' is the temporal Fourier transform of the pertur-
 48 bation of pressure, ψ an envelope function, \mathcal{H}_0^1 the zeroth-order Hankel function of the first
 49 kind, $k_0 = \omega/c_0$ a reference wavenumber computed with respect to a reference speed of sound

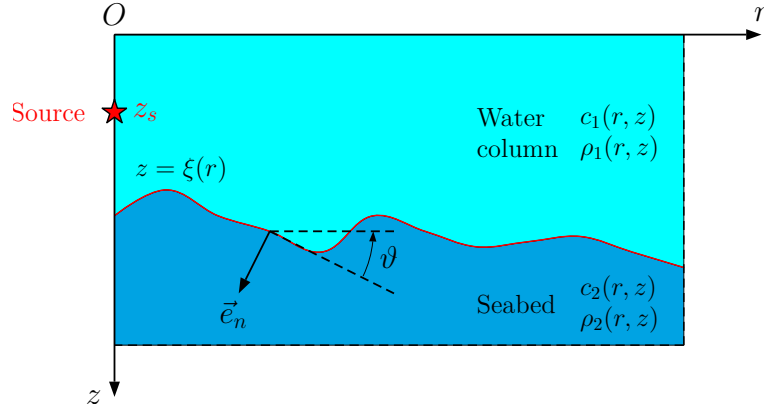


Fig. 1. Sketch of the problem

50 c_0 and ω the angular frequency. Finally, the term $\varepsilon = c_0/c$ represents the index of refraction,
 51 where c is the speed of sound.

52 At the interface $z = \xi(r)$ between the water column and the seabed, two conditions
 53 must be satisfied: the continuity of pressure and the continuity of the normal component of
 54 the particle velocity, which can be expressed in terms of the envelope function ψ as (see also
 55 [Lee and McDaniel \(1988\)](#))

$$\psi^- = \psi^+, \quad (2a)$$

56

$$\psi_z^- - \psi_r^- \xi_r + k_0 \psi^- \frac{\mathcal{H}_1^{(1)}(k_0 r)}{\mathcal{H}_0^{(1)}(k_0 r)} \xi_r = \frac{\rho^-}{\rho^+} \left[\psi_z^+ - \psi_r^+ \xi_r + k_0 \psi^+ \frac{\mathcal{H}_1^{(1)}(k_0 r)}{\mathcal{H}_0^{(1)}(k_0 r)} \xi_r \right], \quad (2b)$$

57 where ρ is the density of the medium, \mathcal{H}_1^1 is the first-order Hankel function of the first kind
 58 and the superscripts \pm indicate the limits $\lim_{z \rightarrow \xi(r)^\pm}$ for a given range r .

59 3. An IIM method for the standard parabolic equation

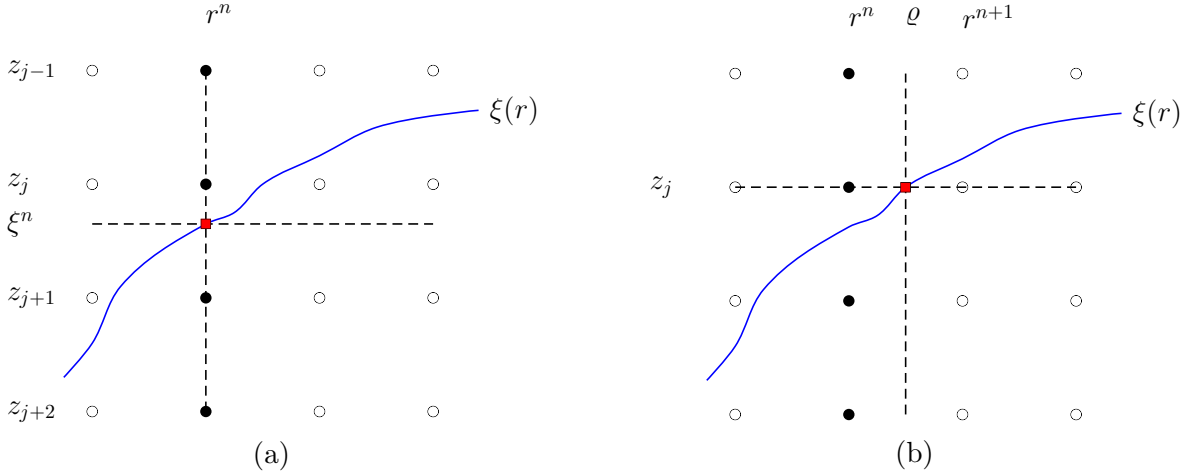


Fig. 2. Seabed interface immersed in the computational grid. Intersection between the interface and (a) the radial direction or (b) the vertical axis.

A uniform mesh $r^n = n\Delta r$, $z_j = j\Delta z$, with $n = 0, 1, \dots, N_r$, $j = 0, 1, \dots, N_z$, is employed, where Δr and Δz are the step sizes in the radial and vertical directions respectively. In what follows, the subscript j and the superscript n will be used to refer to point (r^n, z_j) . In the present approach, the bathymetry is “immersed” in the computational domain and, as schematically illustrated in Fig. 2(a) and Fig. 2(b), might cross the grid both in the radial direction and on the vertical axis. To introduce the new technique, a node (r^n, z_j) away from the interface is first considered. At this regular mesh point, the second derivative $\psi_{zz,j}^n$ is approximated through the standard second order finite difference scheme

$$\psi_{zz,j}^n = \sum_{m=-1}^1 b_m \psi_{j+m}^n, \quad \text{with} \quad b_{-1} = b_{+1} = \frac{1}{\Delta z^2}, \quad b_0 = -\frac{2}{\Delta z^2},$$

and the solution ψ_j^{n+1} at range r^{n+1} is integrated using the Crank-Nicolson method

$$\frac{\psi_j^{n+1} - \psi_j^n}{\Delta r} = \frac{1}{2} [\mathcal{F}_j^n + \mathcal{F}_j^{n+1}].$$

60 The resulting algorithm is second order accurate both in depth and in range. Nevertheless,
 61 at nodes (r^n, z_j) close to the seafloor, the aforementioned schemes cannot be employed. As
 62 described in the following two paragraphs, their coefficients are then modified in such a
 63 way that the unknown function satisfies not only the governing equation but also the jump
 64 conditions.

65 3.1 Range-marching

Let $\varrho \in [r^n, r^{n+1}[$ be the interface position on the line $z = z_j$. To integrate the solution ψ_j
 between ranges r^n and r^{n+1} , Li (1997) elaborated the following first-order accurate scheme

$$\frac{\psi_j^{n+1} - \psi_j^n}{\Delta r} - Q_j^{n+1/2} = \frac{1}{2} (\mathcal{F}_j^{n+1} + \mathcal{F}_j^n),$$

66 where the correction term $Q_j^{n+1/2}$ is given by

$$Q_j^{n+1/2} = -\frac{r^n + \Delta r/2 - \varrho}{\Delta r} \xi_r(\varrho) \times \begin{cases} +\psi_{z,j}^{n+1} - \psi_{z,j}^n & \xi^n \geq \xi^{n+1} \\ -\psi_{z,j}^{n+1} + \psi_{z,j}^n & \xi^n < \xi^{n+1} \end{cases}. \quad (3)$$

67 Depending on the interface location along the vertical axis, the first derivatives appearing
 68 in Eq. (3) are computed using a standard or a modified finite difference scheme.

69 3.2 Depth derivative

70 Let $\xi^n \in [z_j, z_{j+1}[$ be the interface position at range r^n (cf. Fig. 2(b)). As previously
 71 mentioned, modified standard finite difference methods, which take into account the jump
 72 conditions, are needed at the irregular nodes z_j and z_{j+1} . In what follows, the derivation of
 73 such methods shall be treated in details only for the grid point z_j . To begin with, schemes
 74 for the derivatives $\psi_{z,j}^n$ and $\psi_{zz,j}^n$ are sought in the forms $\psi_{z,j}^n = \sum_{m=-1}^1 a_m^{(n,j)} \psi_{j+m}^n$ and

75 $\psi_{zz,j}^n = \sum_{m=-1}^1 b_m^{(n,j)} \psi_{j+m}^n$. Second, up to first order accuracy, the terms $\psi_{z,j}^n$ and $\psi_{zz,j}^n$ can be
 76 written as $\psi_{z,j}^n = \psi_z^{n-} + \mathcal{O}(\Delta z)$ and $\psi_{zz,j}^n = \psi_{zz}^{n-} + \mathcal{O}(\Delta z)$. As a consequence, determining
 77 the $a_m^{(n,j)}$ s and the $b_m^{(n,j)}$ s amounts to expressing ψ_z^{n-} and ψ_{zz}^{n-} as functions of the grid values
 78 $\psi_{j-1}, \psi_j, \psi_{j+1}$. Since ψ_z^{n-} and ψ_{zz}^{n-} are linked to the eight jump values $\psi^{n\pm}, \psi_z^{n\pm}, \psi_r^{n\pm}, \psi_{zz}^{n\pm}$,
 79 eight equations are required to compute the unknowns $\psi^{n\pm}, \psi_z^{n\pm}, \psi_r^{n\pm}, \psi_{zz}^{n\pm}$. Two relations
 80 are provided by the jump conditions (2a) and (2b),

$$\psi^{n-} = \psi^{n+}, \quad (4a)$$

$$\psi_z^{n-} - \xi_r^n \psi_r^{n-} + k_0 \frac{\mathcal{H}_1^{(1)}(k_0 r^n)}{\mathcal{H}_0^{(1)}(k_0 r^n)} \xi_r^n \psi^{n-} = \frac{\rho^{n-}}{\rho^{n+}} \left[\psi_z^{n+} + \xi_r^n \psi_r^{n+} + k_0 \frac{\mathcal{H}_1^{(1)}(k_0 r^n)}{\mathcal{H}_0^{(1)}(k_0 r^n)} \xi_r^n \psi^{n+} \right]. \quad (4b)$$

81 According to Li (1997), a supplementary expression can be obtained by deriving Eq. (2a)
 82 with respect to r . Using the chain rule, it follows that

$$\psi_r^{n-} + \xi_r^n \psi_z^{n-} = \psi_r^{n+} + \xi_r^n \psi_z^{n+}. \quad (5)$$

83 Furthermore, Eq. (1) must be satisfied on both sides of the interface, *i.e.*

$$\psi_r^{n-} = \mathcal{F}^-, \quad (6a) \quad \psi_r^{n+} = \mathcal{F}^+ \quad (6b)$$

85 The last three equations are given by the following truncated Taylor expansions

$$\psi_{j-1}^n = \psi^{n-} + (z_{j-1} - \xi^n) \psi_z^{n-} + \frac{1}{2} (z_{j-1} - \xi^n)^2 \psi_{zz}^{n-}, \quad (7a)$$

$$\psi_j^n = \psi^{n-} + (z_j - \xi^n) \psi_z^{n-} + \frac{1}{2} (z_j - \xi^n)^2 \psi_{zz}^{n-}, \quad (7b)$$

$$\psi_{j+1}^n = \psi^{n+} + (z_{j+1} - \xi^n) \psi_z^{n+} + \frac{1}{2} (z_{j+1} - \xi^n)^2 \psi_{zz}^{n+}. \quad (7c)$$

86 Finally, solving the system (4-5-6-7) allows to express the terms ψ_z^- and ψ_{zz}^- as functions of
 87 the grid values $\psi_{j-1}, \psi_j, \psi_{j+1}$ and thus to identify the coefficients $a_m^{(n,j)}, b_m^{(n,j)}$, $m = -1, \dots, 1$.

88 In a similar manner, the derivatives $\psi_{z,j+1}^n$ and $\psi_{zz,j+1}^n$ at node z_{j+1} are computed as
 89 $\psi_{z,j+1}^n = \psi_z^{n+} = \sum_{m=0}^2 a_m^{(n,j+1)} \psi_{j+m}^n$ and $\psi_{zz,j+1}^n = \psi_{zz}^{n+} = \sum_{m=0}^2 b_m^{(n,j+1)} \psi_{j+m}^n$. The coeffi-
 90 cients $a_m^{(n,j+1)}, b_m^{(n,j+1)}$, $m = 0, \dots, 2$ are determined from a linear system analogous to the
 91 previous one, where Eq. (7a) is replaced by a Taylor expansion for the term ψ_{j+2}^n .

92 It is worth emphasizing that, since the interface position $\xi(r)$ depends on the range r ,
 93 the terms $a_m^{(n,j)}, b_m^{(n,j)}$, $m = -1, \dots, 1$, and $a_m^{(n,j+1)}, b_m^{(n,j+1)}$, $m = 0, \dots, 2$, must be computed
 94 at each step n .

95 It is also worth noting that, although the local truncation error near the bottom
 96 becomes one order lower than at regular points, the global second order accuracy of the
 97 solution remains unaffected (Li, 1997).

98 To conclude, as in the IFD method, the implicit finite-difference equations which are
 99 obtained at grid points away from and close to the seafloor can be recast into a tridiagonal
 100 form, allowing standard fast linear solver to be employed. In addition, it is straightforward
 101 (although tedious) to show that the present numerical algorithm reduces to the IFD method
 102 in the case of an horizontal interface located on the line $z = z_j$.

103 4. Example of application

104 In order to show the capabilities of the new approach, the second wedge problem proposed
 105 by Jensen and Ferla (1990) and graphically illustrated in Fig. 3 is solved. The environment
 106 consists of a homogeneous water column ($c_1 = 1500 \text{ m.s}^{-1}$, $\rho_1 = 1000 \text{ kg.m}^{-3}$), limited above
 107 by a pressure-release flat sea surface ($\psi(r, 0) = 0$) and below by a sloping seafloor. The water
 108 depth is equal to 200 m at the source position and decreases to zero at 4 km range. The
 109

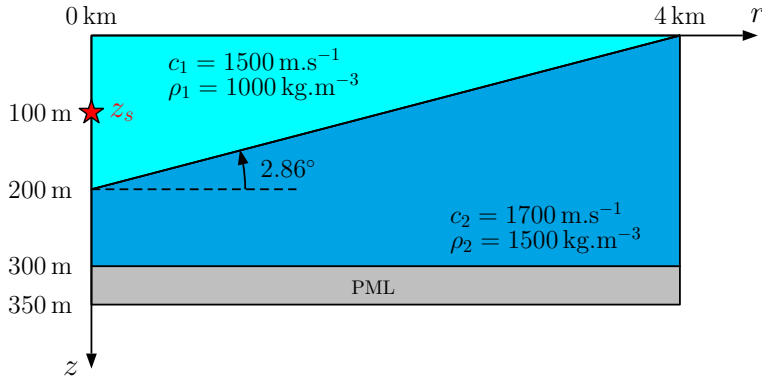


Fig. 3. Test environment

110 bottom is modeled as a homogeneous fluid half-space with a sound speed of $c_2 = 1700 \text{ m.s}^{-1}$
 111 and a density of $\rho_2 = 1500 \text{ kg.m}^{-3}$. A source of frequency equal to $f = 25 \text{ Hz}$ is placed at
 112 $z_s = 100 \text{ m}$ depth. Finally, the Gaussian starter $\psi(0, z) = \sqrt{k_0} e^{-k_0^2(z-z_s)^2/2}$ is used (Jensen
 113 *et al.*, 2011), where the reference wavenumber k_0 is defined with respect to the speed of sound
 114 in the water column, $k_0 = 2\pi f/c_1$. The computational domain is truncated at $D = 350 \text{ m}$
 115 depth by a pressure-release false bottom ($\psi(r, D) = 0$). In order to avoid spurious reflections,
 116 the PML technique developed by Lu and Zhu (2007) is employed. The absorbing layer is
 117 located below 300 m depth. Finally, for the present calculations, the grids steps Δr and Δz
 118 are both set equal to 1 m .

120 As an illustration, the envelope function $\psi(r, z)$ is displayed in Fig. 4. Acoustic energy
 121 penetrates into the bottom at short ranges, where the incidence angle of the beam on the
 122 interface is close to $\pi/2$, and around 3.5 km . Besides, the PML technique clearly proves to be
 123 effective: in the PML layer, outgoing waves are absorbed without generating spurious reflec-
 124 tions toward the water column. The transmission losses $\text{TL}(r, z) = -20 \log_{10}(|\psi(r, z)|/\sqrt{r})$

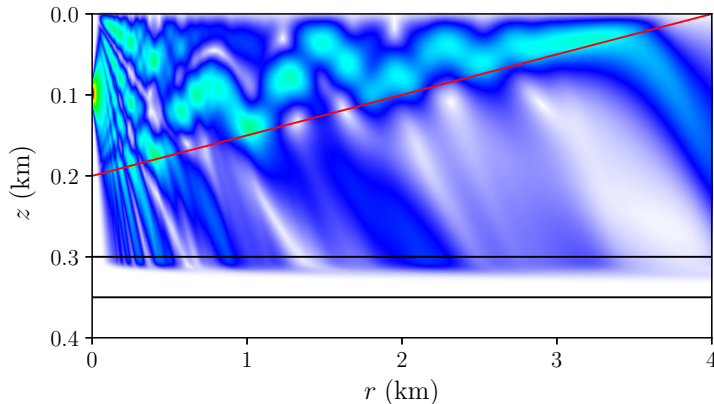


Fig. 4. Envelope function $\psi(r, z)$.

125 computed at 30 m and 150 m depth are plotted in Fig. 5(a) and Fig. 5(b) respectively, along
 126 with the curves obtained by a coordinate rotation (Collins, 1990) and using a standard
 127 stair-step approximation of the bottom. At both depth, a very good agreement with the
 128 reference solution determined with the rotated PE equation is observed, which means that,
 129 as expected, the present results are not affected by energy losses.

130 5. Conclusion

131 A novel approach for the correct treatment of irregular fluid-fluid interfaces in parabolic
 132 wave equation models has been presented. The proposed technique is intrinsically energy-
 133 conserving and allows to consider generic range-dependent ocean floors. It is based on the
 134 immersed interface method, which consists in modifying the numerical algorithm in such a
 135 way that the acoustic field near an interface satisfies not only the governing equation but
 136 also the jump conditions. The present approach has been derived for the standard parabolic
 137 equation and has been validated with a well-known test case. This work represents a first

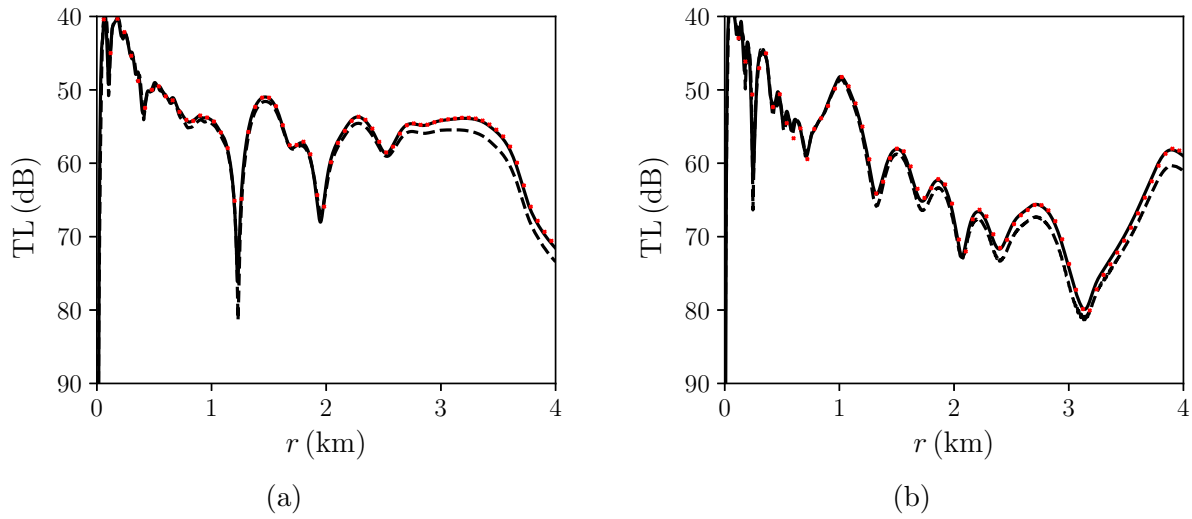


Fig. 5. Transmission loss at (a) $z = 30$ m and (b) $z = 150$ m: present results (solid lines), results obtained with a stair-step approximation (dashed lines), solution computed from a rotated equation (red crosses).

138 step toward the development of a new methodology for the proper handling of irregular
 139 bottoms in the context of generic wide-angle parabolic equations.

140 Acknowledgments

141 The authors would like to thank Dr. Bruno Lombard for fruitful discussions.

142 References and links

143 ¹The partial derivative of a function ψ with respect to a variable r is denoted by ψ_r .

144

145 Collins, M. D. (1990). “The rotated parabolic equation and sloping ocean bottoms,” J.
 146 Acoust. Soc. Am. **87**(3), 1035–1037.

- 147 Collins, M. D., and Westwood, E. K. (1991). “A higher-order energy-conserving parabolic
148 equation for range-dependent ocean depth, sound speed, and density,” *J. Acoust. Soc. Am.*
149 **89**(3), 1068–1075.
- 150 Jensen, F. B., and Ferla, C. M. (1990). “Numerical solutions of range-dependent benchmark
151 problems in ocean acoustics,” *J. Acoust. Soc. Am.* **87**(4), 1499–1510.
- 152 Jensen, F. B., Kuperman, W. A., Porter, M. B., and Schmidt, H. (2011). *Computational*
153 *Ocean Acoustics* (Springer, New York).
- 154 Lee, D., and McDaniel, S. T. (1988). *Ocean acoustic propagation by finite difference method*
155 (Pergamon Press).
- 156 LeVeque, R. J., and Li, Z. (1994). “The immersed interface method for elliptic equations
157 with discontinuous coefficients and singular sources,” *SIAM J. Numer. Anal.* **31**(4), 1019–
158 1044.
- 159 Li, Z. (1997). “Immersed interface methods for moving interface problems,” *Numerical Al-*
160 *gorithms* **14**(4), 269–293.
- 161 Lu, Y. Y., and Zhu, J. (2007). “Perfectly matched layer for acoustic waveguide modeling —
162 benchmark calculations and perturbation analysis,” *CMES* **22**(3), 235–247.
- 163 Metzler, A. M., Moran, D., Collis, J. M., Martin, P. A., and Siegmann, W. L. (2014). “A
164 scaled mapping parabolic equation for sloping range-dependent environments,” *J. Acoust.*
165 *Soc. Am.* **135**(3), EL172–EL178.
- 166 Xu, C.-X., Tang, J., Piao, S.-C., Liu, J.-Q., and Zhang, S.-Z. (2016). “Developments of
167 parabolic equation method in the period of 2000-2016,” *Chin. Phys. B* **11**(2), 1–12.